

SUPPORTING INFORMATION

A Photoelectrocatalytic System as a Reaction Platform for Selective Radical–Radical Coupling

Sunghwan Won,¹ Dongmin Park,² Yousung Jung,^{*3} Hyunwoo Kim,^{*4,5} and Taek Dong Chung^{*1,6}

¹Department of Chemistry, Seoul National University, Seoul 08826, Republic of Korea.

²Department of Chemical and Biomolecular Engineering, Korea Advanced Institute of Science and Technology (KAIST), Daejeon 34141, Republic of Korea.

³Department of Chemical and Biological Engineering, Institute of Chemical Processes, Seoul National University, Seoul 08826, Republic of Korea.

⁴Department of Chemistry, Pohang University of Science and Technology (POSTECH), Pohang 37679, Republic of Korea.

⁵Institute for Convergence Research and Education in Advanced Technology (I-CREATE), Yonsei University, Seoul 03722, Republic of Korea.

⁶Advanced Institutes of Convergence Technology, Suwon-Si, Gyeonggi-do 16229, Republic of Korea.

SUPPORTING INFORMATION

Table of Contents

Table of Contents	2
General Information.....	3
Synthesis and Characterization of the Photoelectrode	4
Procedures for Band Structure Determination	5
General Procedures for Photoelectrocatalytic and Electrochemical Trifluoromethylation of Arenes	7
Procedures for Voltammetric Studies	8
Mechanistic Investigations.....	9
Possible Impact of Surface States.....	11
Computational Details	12
Spectral Data for Products Newly Obtained in This Study	20
References.....	27

SUPPORTING INFORMATION

General Information

All reactions were performed in oven-dried two-neck glass tubes unless otherwise noted. Commercially available reagents were purchased from Sigma Aldrich, Alfa Aesar, Acros, and TCI and used without further purification. Reaction mixtures were purged with N₂ gas for 15 minutes before the reactions began.

Electrolysis experiments were conducted using an MPG-2 multi-potentiostat (Biologic). Kessil PR160 blue LED ($\lambda = 456$ nm) is used as a light source. Carbon felt was purchased from Fuel Cell Store. (Photo)electrochemical experiments were conducted using a Gamry Reference 600 potentiostat (Gamry Instruments). For electrochemical measurements with a 3-electrode configuration, the working-electrode potential was referenced to the Ag/Ag⁺ reference electrode comprised of 0.1 M tetrabutylammonium perchlorate (TBAClO₄) and 10 mM AgNO₃ in MeCN. The potential values are expressed with respect to the Ag/Ag⁺ reference electrode unless otherwise mentioned.

Proton nuclear magnetic resonance (¹H NMR) spectra was recorded on 500 MHz, carbon nuclear magnetic resonance (¹³C NMR) spectra was recorded on 126 MHz, and fluorine nuclear magnetic resonance (¹⁹F NMR) was recorded on 377 MHz by Bruker 500 MHz NMR. Chemical shifts for protons are reported in parts per million (ppm) downfield from tetramethylsilane and are referenced to residual protium in the NMR solvent (CHCl₃ = δ 7.26). Chemical shifts for carbon are reported in parts per million downfield from tetramethylsilane and are referenced to the carbon resonances of the solvent (CDCl₃ = δ 77.16). Data are represented as follows: chemical shift, multiplicity (br. = broad, s = singlet, d = doublet, t = triplet, q = quartet, m = multiplet), coupling constants in Hertz (Hz), integration. High-resolution mass spectra (HRMS) were recorded on a Orbitrap Exploris 120 at Seoul National University.

Abbreviations: Me—methyl, Et—ethyl, Ac—acetyl, Ph—phenyl, EA—ethyl acetate, DCM—dichloromethane, MeCN—acetonitrile, TBA—tetrabutylammonium, DMSO—dimethyl sulfoxide, Boc—*tert*-butyloxycarbonyl.

SUPPORTING INFORMATION

Synthesis and Characterization of the Photoelectrode

Hematite photoelectrodes were synthesized according to the previously reported procedure.^{1,2} Briefly, cleaned fluorine-doped tin oxide (FTO, Solaronix, Switzerland) glass was soaked in a precursor solution containing 0.15 M FeCl₃ and 1.0 M NaNO₃, and enclosed with stainless steel autoclave. The temperature of the system was raised to 95 °C and kept for 4 hours to form β-FeOOH film on the FTO substrate. After cooled at 4 °C for 45 minutes, the electrodes were sonicated for 3 minutes to remove poorly adsorbed particles. The substrates were then annealed at 550 °C for 2 hours to convert the as-deposited β-FeOOH film into hematite (α -Fe₂O₃) nanowire. Then, the hematite electrodes were additionally annealed at 800 °C for 20 minutes to improve their PEC activity.

The surface morphology was analyzed using a SUPRA 55VP field-emission scanning electron microscope (FESEM; Carl Zeiss, Germany) operating at 2 keV at the National Instrumentation Center for Environmental Management at Seoul National University.

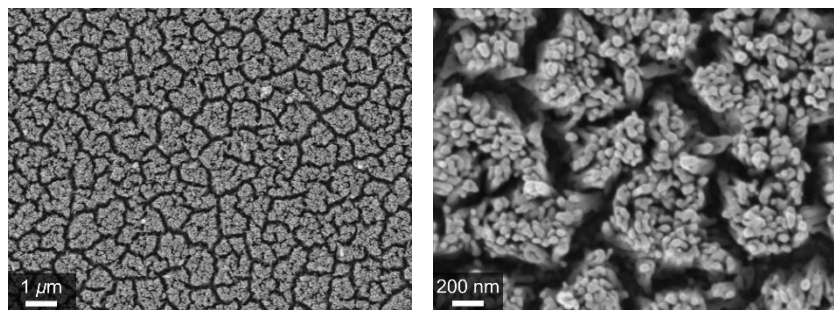


Figure S1. SEM images of a hematite photoanode with different magnification.

The X-ray diffraction (XRD) patterns of the FTO and hematite electrodes were obtained using a D8 Advance X-ray diffractometer (Bruker, Billerica, MA) at the Research Institute of Advanced Materials at Seoul National University.

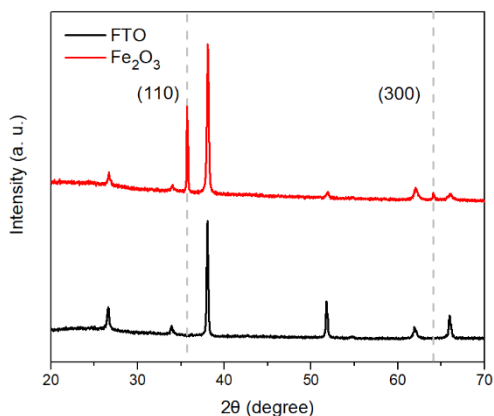


Figure S2. XRD spectra of a bare FTO substrate (black) and a hematite photoelectrode (red). The diffraction peaks corresponding to (110) and (300) faces were observed.

Both SEM images and XRD spectra are in accordance with previously reported ones.^{1,2}

SUPPORTING INFORMATION

Procedures for Band Structure Determination

The band structure of a hematite photoanode was determined by combining the results from UV-Vis diffuse reflectance spectroscopy (UV-Vis DRS), Kelvin probe microscopy (KPFM), and X-ray photoelectron spectroscopy (XPS).

UV-Vis DRS spectra were obtained using a V-770 UV-Visible/NIR spectrophotometer (Jasco, Japan) at the Research Institute of Advanced Materials at Seoul National University. Tauc plot is constructed to get a band-gap value, estimating an indirect bandgap for hematite.

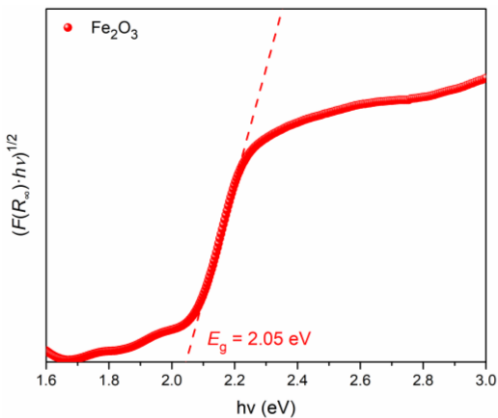


Figure S3. Tauc plot of a hematite photoanode obtained from a UV-vis DRS spectrum. $E_g = 2.05$ eV.

XPS was conducted using AXIS Supra X-ray photoelectron spectrometer (Kratos Analytical, UK) at the National Center for Inter-university Research Facilities (NCIRF) at Seoul National University. Valence electron energy, which corresponds to the difference between the Fermi level and the valence band maximum of the semiconducting material, is obtained from the spectrum. The onset point at 1.28 eV is originated from pinning of the valence band edge at the polaron state.³

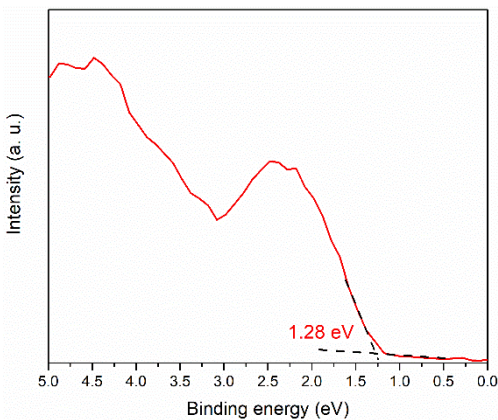


Figure S4. An XPS spectrum of a hematite photoanode and its valence electron energy.

By combining the values obtained above ($E_g = 2.05$ eV, binding energy = 1.28 eV), the work function of undoped hematite (ca. 5.4 eV)³ and the fact that the absolute electrode potential (i.e. the potential value with respect the vacuum) is 4.44 V more positive than the potential relative to the standard hydrogen electrode (SHE), the band structure of hematite is determined as Figure S5. The band positions are well-matched with the previously reported values.⁴⁻⁶ Note that the potential of an Ag/Ag⁺ reference electrode is approximately 550 mV more positive than SHE.

SUPPORTING INFORMATION

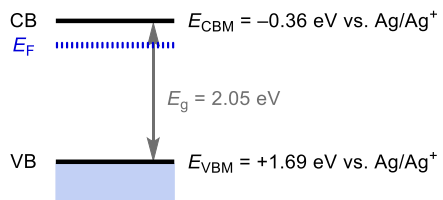


Figure S5. The band structure of a hematite photoanode. CBM = conduction-band minimum, VBM = valence-band maximum. The valence band position is sufficient to oxidize both CF₃SO₂Na and majority of the substrates.

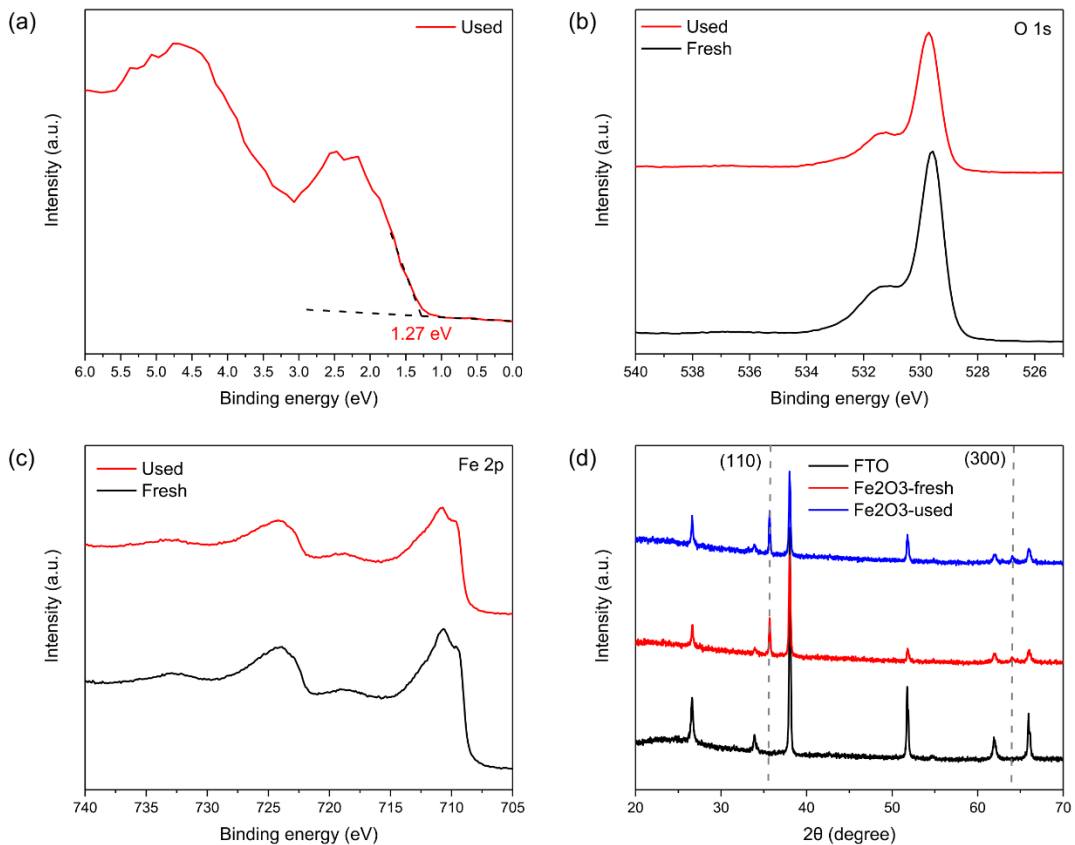
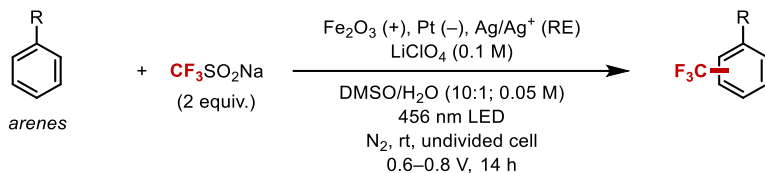


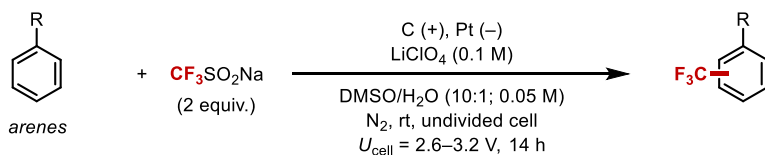
Figure S6. (a-c) XPS spectra of a valence electron, O 1s, and Fe 2p region of a hematite photoanode and (d) XRD spectra after the standard reaction. The spectra are identical to those of the as-synthesized photoanode, indicating that the chemical composition and phase of the hematite surface remain unchanged after running the reaction.

SUPPORTING INFORMATION

General Procedures for Photoelectrocatalytic and Electrochemical Trifluoromethylation of Arenes



Photoelectrocatalytic trifluoromethylation of arenes: An oven-dried, 10 mL two-neck glass tube was equipped with a magnetic stir bar, a rubber septum, a threaded Teflon cap fitted with electrical feed-throughs, a hematite photoanode ($1.0 \times 1.0 \text{ cm}^2$, connected to the electrical feedthrough via a 9 cm in length, 2 mm in diameter graphite rod), a platinum mesh cathode ($0.5 \times 1.0 \text{ cm}^2$), and an Ag/Ag⁺ reference electrode. To this reaction vessel, LiClO_4 (42.5 mg, 0.4 mmol), an arene substrate (0.2 mmol, 1.0 equiv.), and $\text{CF}_3\text{SO}_2\text{Na}$ (62.4 mg, 0.4 mmol, 2 equiv.) were added. The cell was sealed and purged with a nitrogen-filled balloon for 15 minutes. Before initiating the photoelectrocatalytic reaction, a cyclic voltammogram was obtained in the dark to determine the potential range where dark current does not flow. Typical potential-range limit was 0.6–0.8 V, where the initial current was approximately 2 mA. The photoelectrochemical reaction was conducted under illumination with a blue LED (distance ~ 5 cm) at room temperature for 14–18 hours. The reaction mixture was then filtered by silica or Celite and concentrated under reduced pressure. The residue was subjected to flash column chromatography on silica gel (eluted with hexane/ethyl acetate) to yield the desired product.



Electrochemical trifluoromethylation of arenes: An oven-dried, 10 mL two-neck glass tube was equipped with a magnetic stir bar, a rubber septum, a threaded Teflon cap fitted with electrical feed-throughs, a carbon felt anode ($1.0 \times 0.5 \text{ cm}^2$, connected to the electrical feedthrough via a 9 cm in length, 2 mm in diameter graphite rod), and a platinum mesh cathode ($0.5 \times 1.0 \text{ cm}^2$). To this reaction vessel, LiClO_4 (42.5 mg, 0.4 mmol), an arene substrate (0.2 mmol, 1.0 equiv.), and $\text{CF}_3\text{SO}_2\text{Na}$ (62.4 mg, 0.4 mmol, 2 equiv.) were added. The cell was sealed and purged with a nitrogen-filled balloon for 15 minutes. The electrochemical reaction was conducted at a constant cell voltage of 2.6–3.2 V, where the initial current was approximately 2 mA, at room temperature for 14–18 hours. The reaction mixture was then filtered by silica or Celite and concentrated under reduced pressure. The residue was subjected to flash column chromatography on silica gel (eluted with hexane/ethyl acetate) to yield the desired product.

To convert the cell voltage of a two-electrode configuration into the potential of a working electrode in a three-electrode system, a series of potentials were applied to a carbon felt anode in a three-electrode system and the voltage difference between the working electrode and a platinum cathode was measured using a multimeter. The potential of a working electrode under the cell voltage of 2.6–3.2 V in a two-electrode system corresponds to 0.6–0.8 V vs. Ag/Ag⁺ in a three-electrode configuration (Table S1).

Table S1. Potential of a working electrode (E_{WE}) at different cell voltages, with or without a substrate. 50 mM anisole is used as a substrate. Note that E_{WE} slightly decreased over time at a constant cell voltage.

E_{WE} (V vs. Ag/Ag ⁺)	Cell Voltage (V; without a substrate)	Cell Voltage (V; with a substrate)
0.6	2.38	2.5
0.7	2.87	2.89
0.8	3.17	3.24
0.9	3.5	3.57

SUPPORTING INFORMATION

Procedures for Voltammetric Studies

A glassy carbon (GC) rod electrode ($d = 4$ mm) or an FTO glass was used as a working electrode. A platinum wire was used as a counter electrode. Ag/Ag⁺ reference electrode was used as a reference electrode. For an FTO glass, a homemade Teflon electrochemical cell was used, and electrode area was defined by a super-viton P6 O-ring (inner diameter = 5.8 mm; Anyseal, Korea). Scan rate is 50 mV/s, unless otherwise noted.

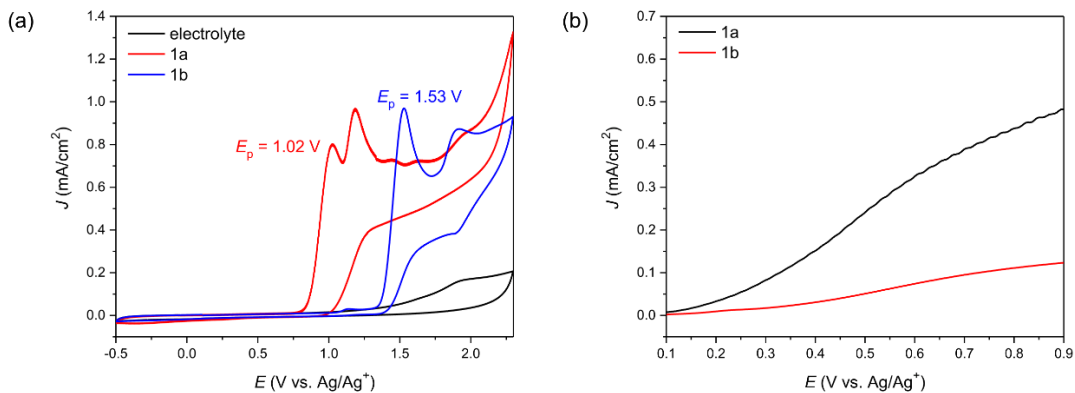


Figure S7. (a) CV of 5 mM **1a** and 5 mM **1b** at a GC electrode. The first anodic peak potential (E_p), which reflects electron density and therefore tendency to be oxidized of the substrate, is acquired from the voltammogram. (b) LSV of 5 mM **1a** and 5 mM **1b** at a hematite photoanode. As anticipated from the higher oxidation potential of **1b** than that of **1a**, the photo-oxidation current of **1b** is significantly smaller than that of **1a** across the entire potential range.

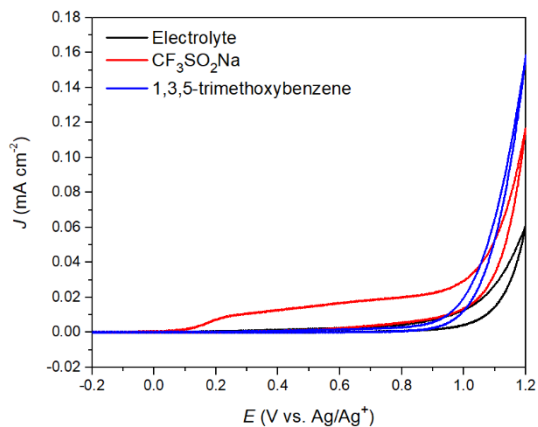


Figure S8. CVs at an FTO electrode. The magnitude of anodic current density is far smaller than that of a GC electrode, indicating the inertness of FTO. The concentration of all substrates is 50 mM, except for CF₃SO₂Na, whose concentration is 100 mM.

SUPPORTING INFORMATION

Mechanistic Investigations

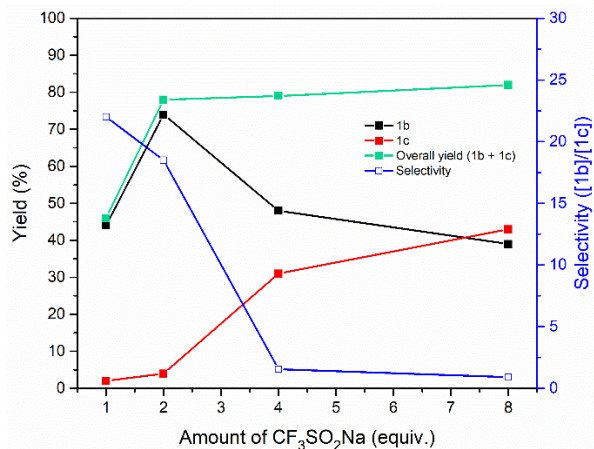


Figure S9. Reaction profile with varying amounts of $\text{CF}_3\text{SO}_2\text{Na}$.

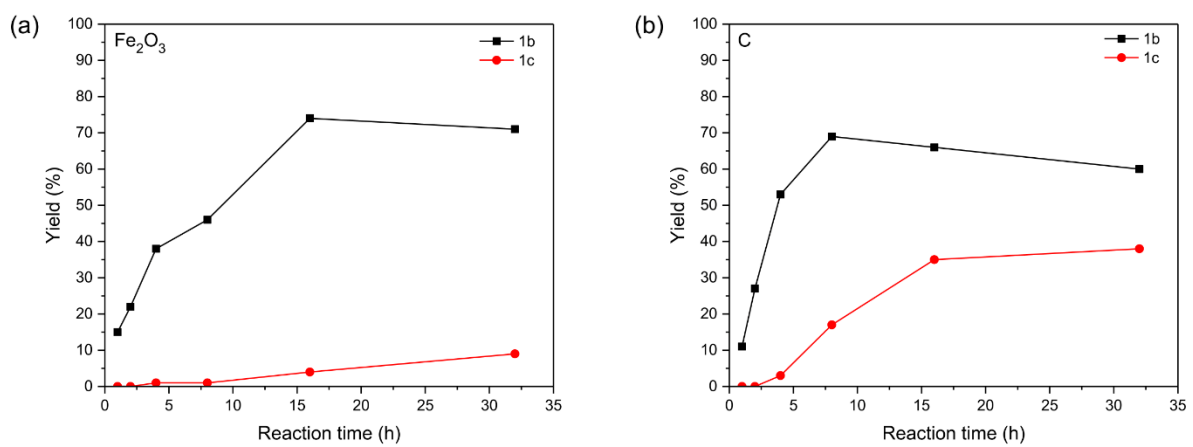


Figure S10. Time-dependent reaction profile at (a) a hematite photoanode and (b) a carbon anode. Even though the mono/bis-selectivity slightly decreases with extended reaction time, the selectivity in the PEC system still outperforms the electrochemical analog at all reaction times.

SUPPORTING INFORMATION

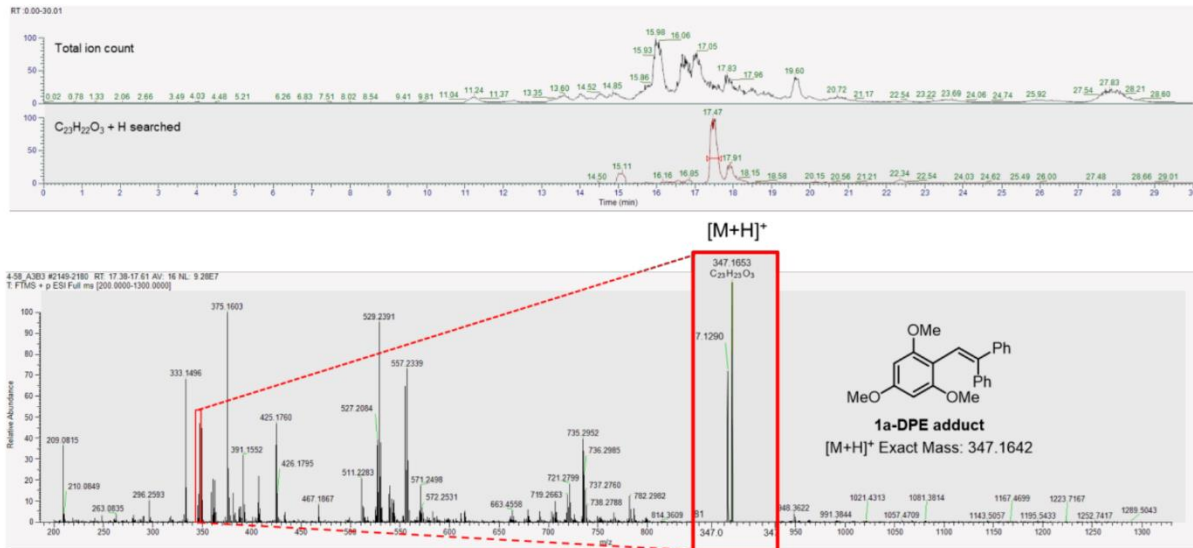
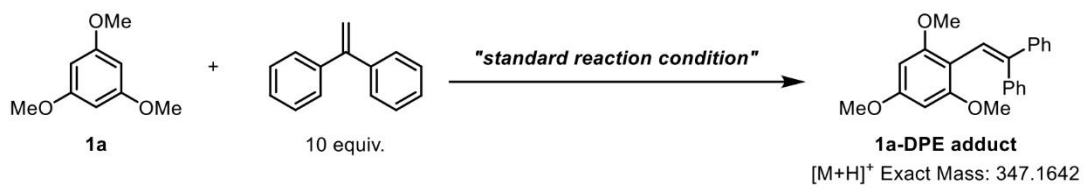


Figure S11. Radical trapping experiment for radical cation intermediate $\mathbf{1a}^+$ and exact mass detection of $\mathbf{1a}$ -DPE adduct in crude mixture. HRMS (ESI) exact mass calculated for $\text{C}_{23}\text{H}_{22}\text{O}_3^+ [\text{M}+\text{H}]^+$ 347.1642, found 347.1653.

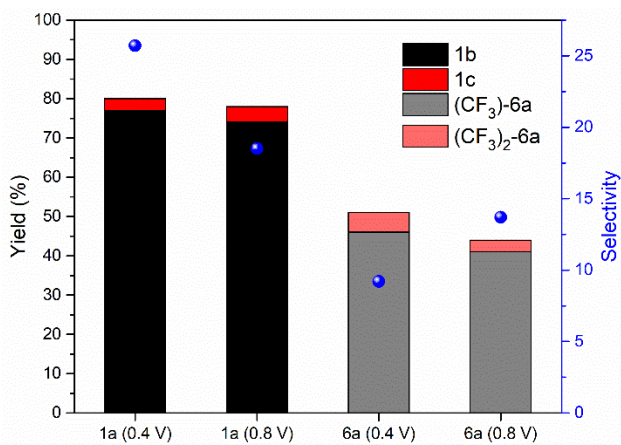


Figure S12. PEC trifluoromethylation of $\mathbf{1a}$ and $\mathbf{6a}$ at different potentials.

SUPPORTING INFORMATION

Possible Impact of Surface States

Presence of surface states is a representative distinctive feature of photoelectrodes compared to conducting electrodes. In the context of energy-related small-molecule activation chemistry, such as oxygen evolution reaction, extensive studies have reported that surface states serve versatile roles, acting as catalytic sites, recombination centers, or mediators of electron transfer, thus significantly influencing the catalytic activity of the system. However, their role in the transformation of organic molecules has not been thoroughly investigated. We propose that the surface states may act as mediation centers for electron transfer, eventually reducing the disparity between the effective overpotential for each oxidation reaction (Figure S9).

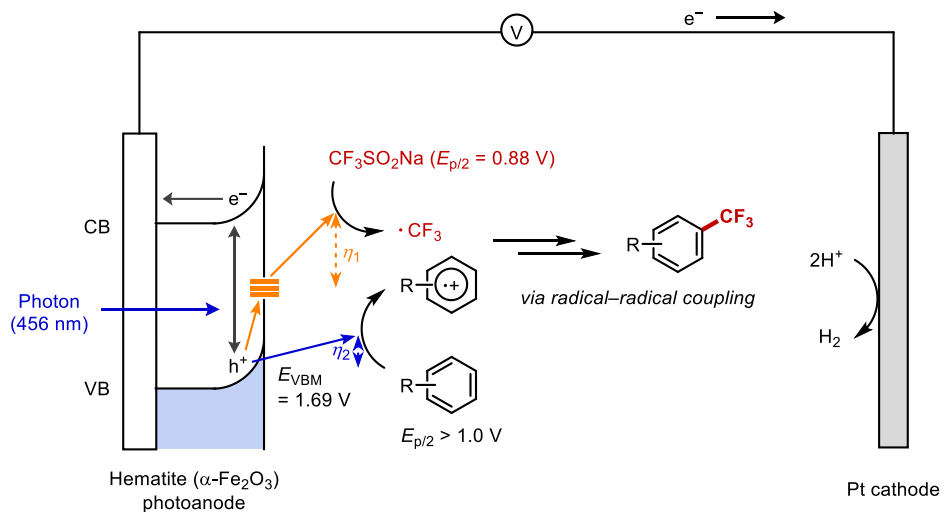


Figure S13. Proposed impact of surface states and corresponding charge-transfer pathway. Surface states can act as electron transfer mediators, consequently decreasing the difference between the effective overpotential for each oxidation reaction, η_1 and η_2 .

SUPPORTING INFORMATION

Computational Details

Density functional theory (DFT) calculations were conducted using Q-Chem 4.4 program⁷ to obtain optimized structures and energies of each reactant, product, transition state, and intermediate species. The range-separated ω B97X-D3 hybrid functional⁸ with the 6-31G* basis set⁹ was used for geometry optimizations and vibrational frequency analysis. Solvation effects were considered using the polarizable continuum model (PCM) as implemented in Q-Chem,¹⁰ with a dielectric constant of 46.7, corresponding to that of DMSO. To obtain the Gibbs free energy, thermal corrections were applied to the single point electron energy obtained on optimized structures with the same functional but with the larger def2-TZVP basis set.¹¹

To account for the potential effects, the computational hydrogen electrode method was applied as in the previously reported case.¹² In the computational hydrogen electrode method, the chemical potential of the electron is referenced to the standard hydrogen electrode (SHE) and the applied potential relative to the SHE.

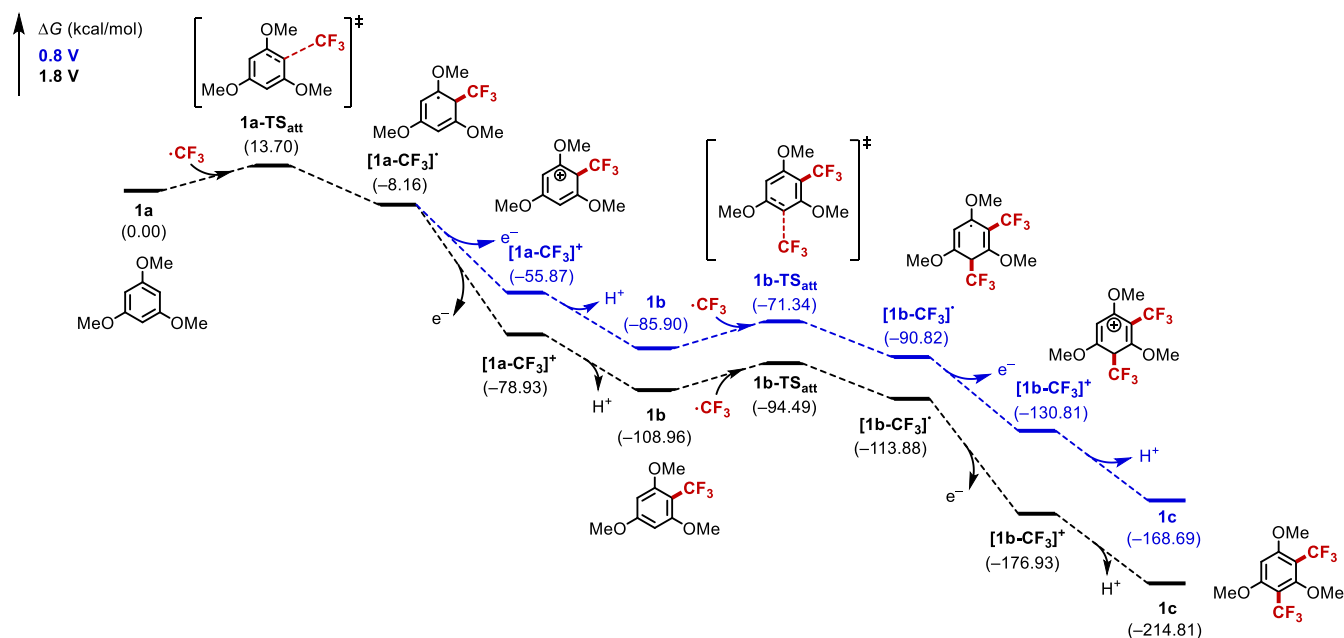


Figure S14. Free energy profile of the radical-attack pathway at 0.8 V (blue) and 1.8 V (black) vs. Ag/Ag⁺. Since the electrode potential only affects the free energy of the oxidation steps, the activation barriers of each substitution step are identical at the different overpotentials. $\Delta G^\ddagger(1\text{a},\text{att}) = 13.69 \text{ kcal/mol}$, $\Delta G^\ddagger(1\text{b},\text{att}) = 14.47 \text{ kcal/mol}$.

SUPPORTING INFORMATION

Energetics for all species involved (in kcal/mol)

	<i>E</i>	Thermal Correction	<i>G</i>
CF₃	-211866.8918	-8.83936495	-211875.7311
1a	-361375.8424	102.4316976	-361273.4107
1a⁺	-361243.1218	101.9708463	-361141.151
[1a-CF₃]⁺	-573182.9701	111.0184818	-573071.9517
[1a-CF₃]⁻	-573265.44	108.1355925	-573157.3031
1a-TS_{att}	-573241.6215	106.1752556	-573135.4462
1b	-572915.7327	103.6047611	-572812.1279
1b⁺	-572774.1335	101.7654674	-572672.368
[1b-CF₃]⁺	-784711.2764	111.5683941	-784599.708
[1b-CF₃]⁻	-784800.5222	107.7470091	-784692.7752
1b-TS_{coup}	-784649.815	108.6967334	-784541.1183
1b-TS_{att}	-784779.4922	106.1070551	-784673.3851
1c	-784450.6169	102.8788523	-784347.738

Cartesian coordinate for all species involved (in angstrom)

CF₃

C -0.0192851414 -0.0192586625 -0.0192442186
 F -0.7659798292 -0.7659991995 0.7755824829
 F -0.7659460154 0.7756309894 -0.7659504904
 F 0.7757168220 -0.7658664714 -0.7658828829

1a

C 1.7293674062 -2.9711038733 -0.0002135663
 O 0.3867297964 -2.5115587896 -0.0004083921
 C 0.1688804044 -1.1718856854 -0.0003077315
 C 1.1935485224 -0.2252616720 -0.0002098938
 C 0.8421692141 1.1312282601 -0.0000504647
 O 1.7578734796 2.1336281171 0.0001115266
 C 3.1335204324 1.7851227548 0.0004667302
 C -0.4894203849 1.5335103974 -0.0000276440
 C -1.4945340671 0.5627696577 -0.0001280242
 O -2.7659763566 1.0394491333 -0.0000110016
 C -3.8272564895 0.0971661305 0.0001148434
 C -1.1777897474 -0.7937781814 -0.0002871405
 H 2.2632468621 -2.6326818844 -0.8956629433
 H 1.6738881189 -4.0601157535 -0.0002891454
 H 2.2629380758 -2.6327776098 0.8954568657
 H 2.2299921565 -0.5334325026 -0.0002656380
 H 3.6771096442 2.7302384251 0.0010528656
 H 3.3984977139 1.2102143417 0.8954493900
 H 3.3991563186 1.2109701461 -0.8948096869
 H -0.7476538529 2.5868501335 0.0001135420
 H -4.7485811609 0.6807546079 0.0003030049
 H -3.7962892187 -0.5355663677 -0.8944661590
 H -3.7959786028 -0.5356581628 0.8946215256
 H -1.9327680695 -1.5705796498 -0.0003767780

1a⁺

C 1.7183836072 -3.0171292293 -0.0002336927
 O 0.3856446693 -2.4709391421 -0.0003834538
 C 0.2000224972 -1.1763460146 -0.0003001694
 C 1.2476698976 -0.2354801687 -0.0001762230
 C 0.8965216419 1.0983666326 -0.0000147951
 O 1.7363565097 2.1147849769 0.0002086429
 C 3.1461579619 1.8484963174 0.0004899805
 C -0.4845756001 1.5029064529 -0.0000386630
 C -1.5188143026 0.5319605236 -0.0001393036

SUPPORTING INFORMATION

O -2.7561903699 1.0312386123 -0.0000249986
C -3.8443096174 0.1053385653 0.0001167553
C -1.1845646575 -0.7999316188 -0.0003134725
H 2.2472756015 -2.6987349833 -0.9011159475
H 1.5829627649 -4.0963752301 -0.0003269252
H 2.2470087887 -2.6988464447 0.9008446042
H 2.2798643080 -0.5564740328 -0.0001954553
H 3.6202861284 2.8272988708 0.0009206199
H 3.4212741416 1.2902877876 0.8997106154
H 3.4217480968 1.2908870568 -0.8989580662
H -0.7271562380 2.5602726343 0.0000599086
H -4.7474775346 0.7134466683 0.0003722101
H -3.8146302051 -0.5204032607 -0.8976887988
H -3.8142318722 -0.5205702405 0.8977942811
H -1.9185560220 -1.5965527602 -0.0004315687

[1a-CF₃]⁺

C 5.8937237091 4.1567865635 2.1352230636
F 7.1216452878 3.6341598585 2.1208119520
F 6.0181885605 5.4792910915 2.2579456698
F 5.2604134043 3.6973616051 3.2241516521
C 1.2497765674 0.4972595899 1.4502087874
O 1.4350481556 1.9241478821 1.3557441461
C 2.6143103495 2.4397416933 1.1507360920
C 3.7795895729 1.6493321364 0.9905696424
C 4.9734236081 2.2807594207 0.7902149134
O 6.1185048415 1.6876414678 0.5683935897
C 6.1708019031 0.2499056402 0.5489750839
C 5.1116802133 3.7807812600 0.8543194148
C 3.7902477215 4.5052529617 0.8316217476
O 3.9355560947 5.7922134485 0.6165127629
C 2.7709999745 6.6324241389 0.6394873928
C 2.6147084036 3.8582553480 1.0446751007
H 1.5526688124 0.0203052656 0.5160516527
H 0.1817395700 0.3675764228 1.6114337201
H 1.8142172731 0.1031483280 2.2977400524
H 3.7124304695 0.5706243876 0.9873072560
H 7.2148763823 0.0039532815 0.3684391547
H 5.8456090008 -0.1451067365 1.5144709291
H 5.5411056106 -0.1316467363 -0.2586886491
H 5.7204864139 4.1196306914 0.0086001708
H 3.1377871239 7.6337586233 0.4242447360
H 2.0613333035 6.3135401179 -0.1283992166
H 2.3106690139 6.5983750712 1.6299005702
H 1.6585499357 4.3641185181 1.0774818084

[1a-CF₃]⁻

C 5.8623235337 4.1390368785 2.2729952907
F 7.1034236210 3.6241397312 2.3117789486
F 5.9837095441 5.4653368914 2.4511499456
F 5.1970742492 3.6544540587 3.3368602308
C 1.2610804100 0.5056917231 1.5234833503
O 1.3820187761 1.9175433425 1.4746329375
C 2.6107736074 2.4437147949 1.2176569713
C 3.7805911060 1.6771478227 1.0263397401
C 4.9799511016 2.3083440976 0.8173837462
O 6.1506102139 1.6966103783 0.5131637132
C 6.1347999360 0.2823698034 0.3952648642
C 5.1477199769 3.7981786473 0.9527172779
C 3.8195881548 4.5024701895 0.8614917520
O 3.9684812516 5.8166152682 0.5733210297
C 2.7891307571 6.6019700014 0.4927105592
C 2.6392753158 3.8574957608 1.0694804371

SUPPORTING INFORMATION

H 1.5234447754 0.0509311181 0.5608883556
H 0.2131692304 0.3010080944 1.7465722625
H 1.8914136281 0.0781054258 2.3122249475
H 3.7249116783 0.5961639261 0.9994823546
H 7.1469678297 -0.0120689219 0.1172031166
H 5.8620795848 -0.1860461384 1.3479175252
H 5.4311596232 -0.0367974949 -0.3825256889
H 5.8179056947 4.1700124358 0.1653602877
H 3.1153284853 7.6060572545 0.2210597531
H 2.1086034374 6.2145439578 -0.2746608544
H 2.2736631796 6.6271870814 1.4594164524
H 1.6908925750 4.3833752127 1.0648038897

1a-TS_{att}

C 5.9477076935 4.1639339601 2.5182230704
F 7.1240210895 4.7858203778 2.3686548882
F 5.1367811037 4.9505643708 3.2366074939
F 6.1479644152 3.0291393365 3.1992422795
C 1.2486732638 0.5603966278 1.5945749327
O 1.3763624625 1.9635990464 1.4108695936
C 2.5896578427 2.4623695106 1.0809368698
C 3.7274764881 1.6695158727 0.8974387908
C 4.9284202852 2.2983915774 0.5757316014
O 6.0890791065 1.6426602315 0.3538274125
C 6.0852223056 0.2256809806 0.4552909250
C 5.0277363623 3.7054047890 0.5166248504
C 3.8303791907 4.4601532116 0.5949601794
O 3.9917513313 5.7846508223 0.3843843124
C 2.8477548569 6.6187410582 0.5014598340
C 2.6278193548 3.8565186667 0.9177058307
H 1.4590641051 0.0182738933 0.6658513959
H 0.2119038372 0.3936132739 1.8878359587
H 1.9153014787 0.2044827011 2.3879451565
H 3.6725181060 0.5929735489 0.9837381885
H 7.1072676653 -0.0930760647 0.2498856181
H 5.7952243865 -0.0973682429 1.4613944934
H 5.4081242538 -0.2212770468 -0.2814253969
H 5.9018472951 4.1513028735 0.0528870823
H 3.1944777527 7.6296334107 0.2862990638
H 2.0765083007 6.3338413595 -0.2228160281
H 2.4346009219 6.5793851075 1.5152084557
H 1.7064460216 4.4142660866 1.0348363433

1b

C 6.3314713778 4.5050465785 0.5877087665
F 7.4357938845 3.7567921009 0.4519952714
F 6.2837245196 5.2959243543 -0.5092534730
F 6.5645117525 5.3287876898 1.6360371304
C 1.2326490576 0.4792141691 1.2013559164
O 1.3590636973 1.8952532243 1.1864837548
C 2.5922175417 2.4293989840 1.0586314878
C 3.7550712197 1.6717237274 0.9619221728
C 4.9885535403 2.3197177005 0.8186755846
O 6.1410258285 1.6253629818 0.7279262391
C 6.0939700043 0.2061309983 0.7815277030
C 5.0617336680 3.7225408350 0.7640064575
C 3.8587227173 4.4580293268 0.8761905863
O 3.9889087709 5.8000094838 0.8255134088
C 2.8198073619 6.5998965573 0.9381012812
C 2.6333976365 3.8255597715 1.0230906558
H 1.6291084546 0.0387726818 0.2801763534
H 0.1630748598 0.2790969953 1.2694457463
H 1.7416224720 0.0452276774 2.0690176946

SUPPORTING INFORMATION

H 3.7101631989 0.5928327553 0.9948686914
H 7.1305017627 -0.1237616127 0.7112711287
H 5.6676113297 -0.1443021509 1.7276420240
H 5.5225001769 -0.2047430641 -0.0578672479
H 3.1658523015 7.6312463930 0.8741247650
H 2.1184196814 6.3926664165 0.1228341512
H 2.3238779572 6.4392529066 1.9014623493
H 1.7028168408 4.3728153243 1.1037283964

1b⁺

C 6.3494981368 4.5051532636 0.5509100606
F 7.4275026652 3.7408282248 0.3733449506
F 6.2571502562 5.3054047226 -0.5236856297
F 6.5869977129 5.2854646415 1.6183371573
C 1.1607492732 0.4845623939 1.1908332086
O 1.3711374762 1.9054781829 1.1721671004
C 2.5954845787 2.3689114393 1.0513083384
C 3.7421459745 1.6166786842 0.9544501133
C 4.9708960885 2.2905186002 0.8133269586
O 6.1040299776 1.6550622332 0.7416519499
C 6.1580062960 0.2154753956 0.8125304805
C 5.0556049010 3.7345274968 0.7417209465
C 3.8889271228 4.4755890611 0.8680731835
O 3.9872250045 5.7992621750 0.8306962527
C 2.8106173245 6.6079815302 0.9619194475
C 2.6521489051 3.8062313319 1.0220475047
H 1.5454713413 0.0402617056 0.2692011004
H 0.0820378925 0.3583608063 1.2529792802
H 1.6482326325 0.0476853938 2.0663233625
H 3.7127874289 0.5370947945 0.9859563261
H 7.2175870558 -0.0237119425 0.7629378815
H 5.7334327765 -0.1263868748 1.7583994350
H 5.6283634346 -0.2148637946 -0.0397618346
H 3.1695134156 7.6335532051 0.9036421896
H 2.1121435200 6.4083010924 0.1448409862
H 2.3334119500 6.4376355898 1.9308839897
H 1.7150684725 4.3434334532 1.1115822558

[1b-CF₃]⁺

C 6.2791682384 4.5323515771 0.7555329457
F 7.3659041089 3.7818868905 0.9469710754
F 6.4023253071 5.1025314690 -0.4571317445
F 6.3246098963 5.5212391792 1.6654155054
C 1.1062361223 0.4493956588 0.4275746730
O 1.2864740071 1.8754556221 0.5263817327
C 2.4870416949 2.3603299236 0.6944372179
C 3.6467084732 1.6503985475 0.7649219935
C 4.8782615862 2.3392518193 0.9144689830
O 5.9952174339 1.6927986648 1.0496010455
C 6.0322857626 0.2497900454 1.0874553300
C 4.9729663087 3.7714958811 0.8599516073
C 3.8132733532 4.4949560115 0.7325773485
O 3.8997760083 5.7840332443 0.5362327170
C 2.7943250960 6.5790427446 0.0479433364
C 2.4671959117 3.8450263831 0.9176260401
H 1.6182579608 0.0727275468 -0.4608346828
H 0.0315092507 0.3079252699 0.3384432053
H 1.4837817475 -0.0309626862 1.3331661080
H 3.6424007905 0.5730061680 0.6837734499
H 7.0826166963 0.0060945305 1.2284060320
H 5.4373552525 -0.1129913698 1.9278580031
H 5.6714534141 -0.1544616527 0.1399934248
H 2.4197932263 6.1532628634 -0.8848933803

SUPPORTING INFORMATION

H 2.0095110277 6.6508837164 0.7987807164
H 3.2290088622 7.5591011183 -0.1334487209
H 1.7167157849 4.2912023276 0.2582173995
C 1.9882954124 4.0888056479 2.3758803443
F 2.7373435360 3.3966675469 3.2405315124
F 2.0748603584 5.3812723487 2.7059408162
F 0.7214858169 3.7063009852 2.5179744390

[1b-CF₃]^{*}

C 6.2225092918 4.5475474318 0.6924048217
F 7.3308984021 3.7979528801 0.6213744753
F 6.2018791389 5.2867398705 -0.4375230793
F 6.4121857976 5.4075124236 1.7152396384
C 1.1520481065 0.4566136558 0.3597274213
O 1.2521599838 1.8566448438 0.5870142793
C 2.4798518820 2.3721543151 0.7947946468
C 3.6473157163 1.6724175681 0.8187288070
C 4.8992938029 2.3379737585 0.9232168480
O 6.0640552707 1.6615140400 1.0502521433
C 6.0261007293 0.2420302916 1.0732176980
C 4.9456548210 3.7579975538 0.8532007260
C 3.7726205985 4.4824911630 0.8490612280
O 3.8477567276 5.8357501984 0.8035109434
C 2.9220888099 6.5276385989 -0.0351507333
C 2.4224545055 3.8487131027 1.0563865354
H 1.7243249890 0.1646676796 -0.5280485845
H 0.0927364096 0.2550482012 0.2008550895
H 1.5087153829 -0.1044299767 1.2305938172
H 3.6283317725 0.5958238527 0.7120236010
H 7.0612824341 -0.0788216354 1.1908650046
H 5.4302543314 -0.1258988809 1.9160996326
H 5.6287464896 -0.1616863946 0.1355305648
H 2.9159254456 6.0997253929 -1.0426972202
H 1.9124844512 6.5152830917 0.3855255389
H 3.2804954350 7.5561440366 -0.0757355461
H 1.6694266111 4.2920683853 0.3909803690
C 1.9120249684 4.1334119886 2.4818309268
F 2.7508337127 3.6438268298 3.4097977299
F 1.7952344041 5.4543122246 2.7051864469
F 0.7064680240 3.5876515319 2.7014847043

1b-TS_{coup}

C 6.2248125266 4.6361057180 0.6907014706
F 7.3114896694 3.9012209862 0.9566179819
F 6.4833729660 5.2843661859 -0.4650465638
F 6.1582623116 5.5802915884 1.6546815702
C 1.0953197809 0.5859728072 0.3642440783
O 1.2472298189 1.9990831245 0.2375224660
C 2.4676185994 2.5409805472 0.3963929379
C 3.6027855038 1.8145700248 0.7594374901
C 4.8419593323 2.4674925391 0.8538214645
O 5.9564970610 1.8056599280 1.1984945656
C 5.8741046774 0.4120182537 1.4810073198
C 4.9441438022 3.8482234485 0.6030856413
C 3.7694424709 4.5634089966 0.2751378736
O 3.9219843657 5.8819872916 0.0778376577
C 2.7758310218 6.6614548178 -0.2525032692
C 2.5360010256 3.9259932039 0.1890908876
H 1.7277085849 0.0571577571 -0.3554939160
H 0.0457681451 0.3868779715 0.1500638324
H 1.3299620204 0.2524553545 1.3804495088
H 3.5352785738 0.7491736803 0.9286036566
H 6.8819001066 0.1135135258 1.7679117740

SUPPORTING INFORMATION

H 5.1848621731 0.2188685689 2.3093956153
H 5.5617355484 -0.1503638849 0.5950007398
H 2.3439956885 6.3324222751 -1.2030270545
H 2.0232092918 6.6057380029 0.5406451721
H 3.1392701688 7.6841206237 -0.3433328507
H 1.6283259542 4.4496082760 -0.0828675572
C 2.2578831122 3.3196883739 3.1668720837
F 2.2139289790 2.1306382715 3.5247214196
F 3.3289578527 3.9421010909 3.2380211922
F 1.2025173130 3.9179886747 2.9022612860

1b-TS_{att}

C 6.2793125082 4.5423746652 0.7588663340
F 7.3869906154 3.8224618026 0.9827009989
F 6.4907117337 5.2065094346 -0.4004938285
F 6.2408711677 5.4808087947 1.7311121206
C 1.2062594255 0.4240191398 0.5140294473
O 1.3311956561 1.8382853207 0.4158477429
C 2.5563246491 2.3801596914 0.5346422551
C 3.7212962367 1.6580533717 0.7081572264
C 4.9498543769 2.3341207294 0.8101218678
O 6.1043927020 1.6667271601 0.9869331110
C 6.0763943783 0.2459630021 1.0560314713
C 5.0086427534 3.7393621693 0.7141048356
C 3.8107505282 4.4480756979 0.5174296512
O 3.9192046877 5.7820439414 0.3781190257
C 2.7559171927 6.5435621318 0.0665011730
C 2.5573777437 3.7996534086 0.5412573878
H 1.7412776216 -0.0751898291 -0.3008079356
H 0.1394921273 0.2151359869 0.4342940749
H 1.5800916356 0.0660822703 1.4791710640
H 3.6919267394 0.5786899182 0.7485959818
H 7.1154898966 -0.0608154236 1.1738866672
H 5.4920215441 -0.0962172763 1.9167867565
H 5.6722753700 -0.1864016733 0.1349050069
H 2.3346799314 6.2348508038 -0.8957417965
H 1.9989038795 6.4542022745 0.8511058676
H 3.0967788387 7.5763796259 0.0061492309
H 1.6767353310 4.2894382845 0.1402908506
C 1.7912542804 4.1871303846 2.5658219802
F 1.6443198851 3.0454600156 3.2442657689
F 2.6422123826 4.9765036139 3.2308936192
F 0.6032026272 4.8013885859 2.4947705172

1c

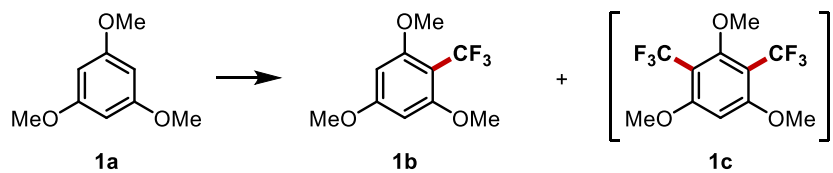
C 6.2757411998 4.4962170863 0.7489960781
F 7.2680731054 3.9238708486 1.4621097258
F 6.6635243124 4.4655033186 -0.5449377938
F 6.2642779332 5.7880055027 1.1078017559
C 1.4289132907 0.2138039141 1.3096316882
O 1.4869370180 1.6140004922 1.5633060523
C 2.6353856014 2.2719719329 1.3410872931
C 3.7928938595 1.6413457428 0.8968926103
C 4.9491999615 2.3900067689 0.6971638680
O 6.0949434536 1.8506903635 0.2531879068
C 6.1309295097 0.4553103677 -0.0346114538
C 4.9678455631 3.7760258151 0.9516434503
C 3.7818873536 4.4003004398 1.3657660348
O 3.7712581846 5.7415741564 1.5926063326
C 3.4707220990 6.5252011863 0.4353188108
C 2.6084203664 3.6616069275 1.5720895777
H 1.6355984463 -0.0016666352 0.2563168805
H 0.4087272639 -0.0833179448 1.5513429036

SUPPORTING INFORMATION

H 2.1287070765 -0.3332265278 1.9491305526
H 3.7949180397 0.5769274521 0.7116325664
H 7.1385964932 0.2593426001 -0.3993299493
H 5.9424695757 -0.1352276382 0.8678803969
H 5.4012040048 0.1984131123 -0.8090199794
H 4.2267907548 6.3757318667 -0.3422416788
H 2.4816014956 6.2686144923 0.0419425617
H 3.4790237376 7.5636499523 0.7658544960
C 1.2976653726 4.2495050282 2.0265558124
F 0.8836744674 3.6973724022 3.1862566054
F 1.3168871092 5.5742986884 2.2312347217
F 0.3203492289 4.0254107600 1.1209236390

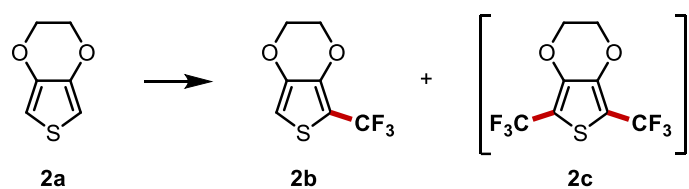
SUPPORTING INFORMATION

Spectral Data for Products Newly Obtained in This Study



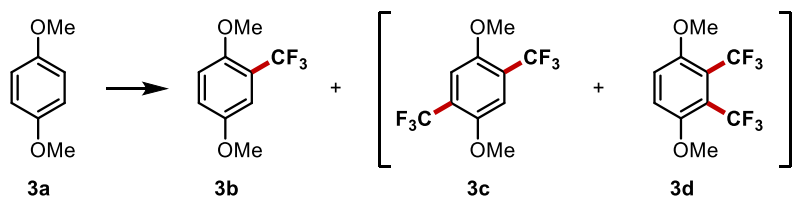
1,3,5-trimethoxy-2-(trifluoromethyl)benzene (1b). Identical to previously reported spectra.¹³

1,3,5-trimethoxy-2,4-bis(trifluoromethyl)benzene (1c). Identical to previously reported spectra.¹³



5-(trifluoromethyl)-2,3-dihydrothieno[3,4-b][1,4]dioxine (2b). Identical to previously reported spectra.¹⁴

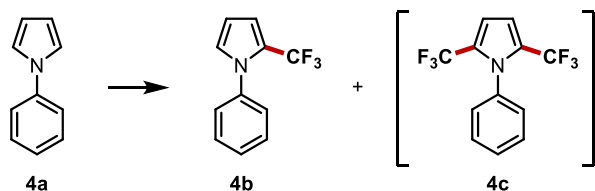
5,7-bis(trifluoromethyl)-2,3-dihydrothieno[3,4-b][1,4]dioxine (2c). Identical to previously reported spectra.¹⁵



1,4-dimethoxy-2-(trifluoromethyl)benzene (3b). Identical to previously reported spectra.¹⁶

1,4-dimethoxy-2,5-bis(trifluoromethyl)benzene (3c). ^1H NMR (500 MHz, CDCl_3) δ 7.22 (s, 2H), 3.90 (s, 6H); ^{13}C NMR (126 MHz, CDCl_3) δ 150.96, 122.87 (q, $^1J_{\text{CF}} = 273.2$ Hz), 122.74 (q, $^2J_{\text{CF}} = 31.5$ Hz), 111.81 (q, $^3J_{\text{CF}} = 5.2$ Hz), 56.91.; ^{19}F NMR (377 MHz, CDCl_3) δ -62.88 (s). Identical to previously reported spectra.¹⁷

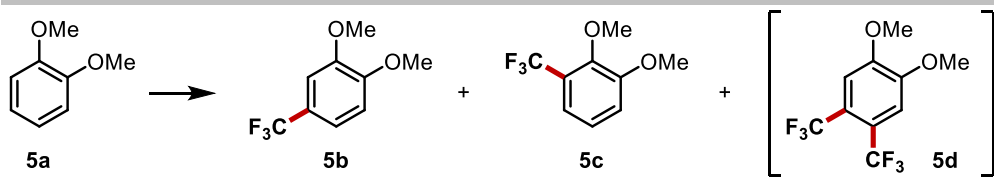
1,4-dimethoxy-2,3-bis(trifluoromethyl)benzene (3d). ^1H NMR (500 MHz, CDCl_3) δ 7.21 (s, 2H), 3.88 (s, 6H); ^{19}F NMR (471 MHz, CDCl_3) δ -55.16 (s). Identical to previously reported spectra.²⁴



1-phenyl-2-(trifluoromethyl)-1H-pyrrole (4b). Identical to previously reported spectra.¹⁸

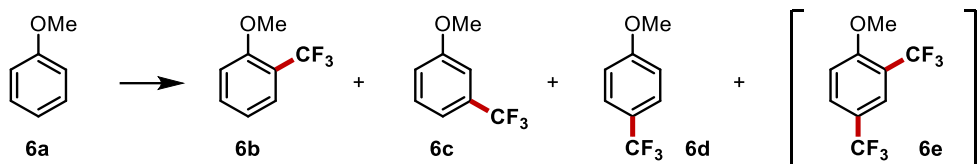
1-phenyl-2,5-bis(trifluoromethyl)-1H-pyrrole (4c). Identical to previously reported spectra.¹⁹

SUPPORTING INFORMATION



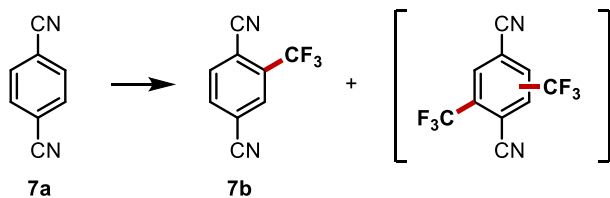
Mono-substituted products (5b–5c). Identical to previously reported spectra.¹⁶

1,2-dimethoxy-4,5-bis(trifluoromethyl)benzene (5d). Identical to previously reported spectra.²⁰



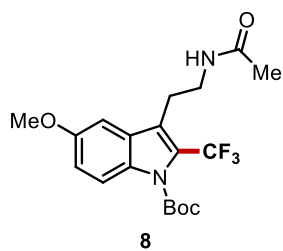
Mono-substituted products(6b–6d). Identical to previously reported spectra.²¹

1-methoxy-2,4-bis(trifluoromethyl)benzene (6e). ^1H NMR (499 MHz, CDCl_3) δ 7.83 (s, 1H), 7.77 (d, $J = 9.1$ Hz, 1H), 7.09 (d, $J = 8.7$ Hz, 1H), 3.97 (s, 3H). ^{19}F NMR (471 MHz, CDCl_3) δ -61.85 (s), -63.10 (s). Identical to previously reported spectra.²⁵

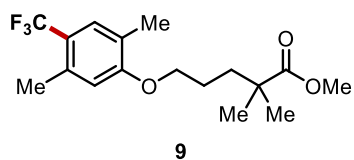


2-(trifluoromethyl)terephthalonitrile (7b). Identical to previously reported spectra.²²

From the ^{19}F NMR data, we integrated the peaks of the suspected bis-substituted product based on the previously reported paper.²² However, since only a trace amount of the product (< 5%) was generated from both the PEC and EC systems and considerable amount of starting material **7a** was left, we could not separate the suspected bis-substituted product. Nevertheless, we want to emphasize that the reaction results of **7a** are consistent with our key scientific observation that the selectivity result of oxidatively demanding substrates, which cannot be oxidized by either PEC or EC systems, is effectively identical in both systems.

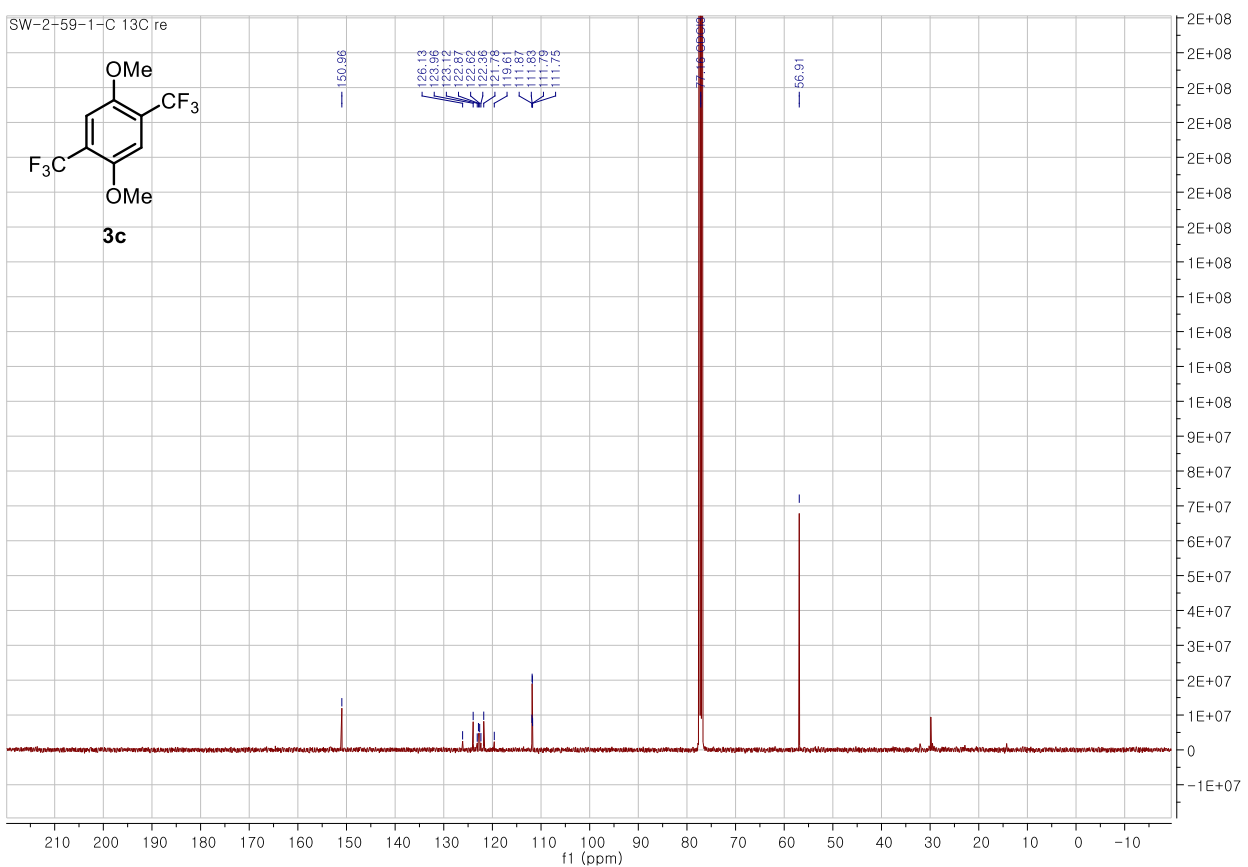
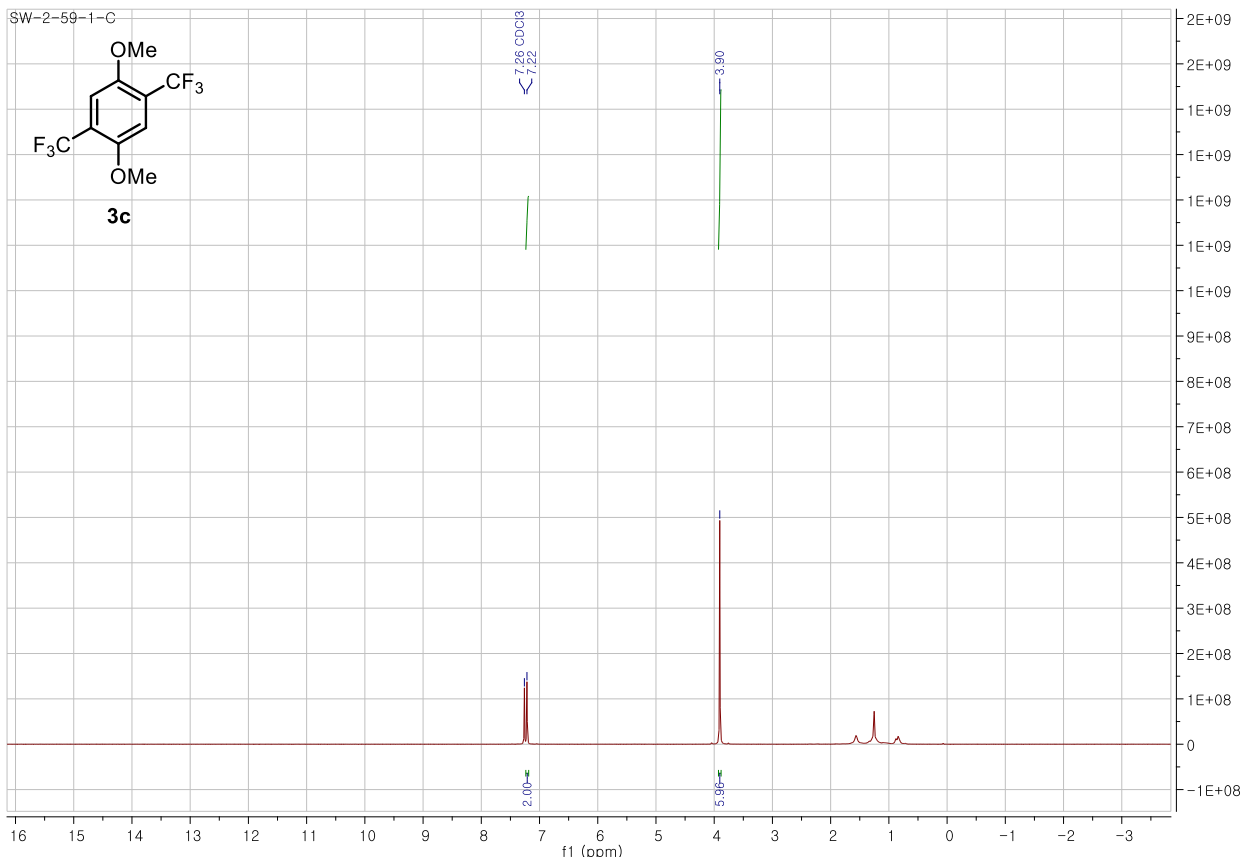


tert-butyl 3-(2-acetamidoethyl)-5-methoxy-2-(trifluoromethyl)-1*H*-indole-1-carboxylate (8). ^1H NMR (500 MHz, CDCl_3) δ 8.05 (d, $J = 9.2$ Hz, 1H), 7.17 (s, 1H), 7.06 (d, $J = 9.1$ Hz, 1H), 5.76 (s, 1H), 3.88 (s, 3H), 3.48 (q, $J = 6.7$ Hz, 2H), 3.11 (t, $J = 6.2$ Hz, 2H), 1.93 (s, 3H), 1.64 (s, 9H). ^{13}C NMR (126 MHz, CDCl_3) δ 170.55, 156.50, 148.95, 131.62, 123.93 (q, $3J_{\text{CF}} = 2.5$ Hz), 128.89, 122.96 (q, $2J_{\text{CF}} = 37.3$ Hz), 121.82 (q, $1J_{\text{CF}} = 269.2$ Hz), 117.38, 116.69, 101.54, 85.33, 55.87, 39.87, 27.93, 24.85, 23.37. ^{19}F NMR (377 MHz, CDCl_3) δ -54.31 (s). HRMS (ESI) exact mass calculated for $\text{C}_{19}\text{H}_{24}\text{F}_3\text{N}_2\text{O}_4^+ [\text{M}+\text{H}]^+$ 401.1683, found 401.1689.

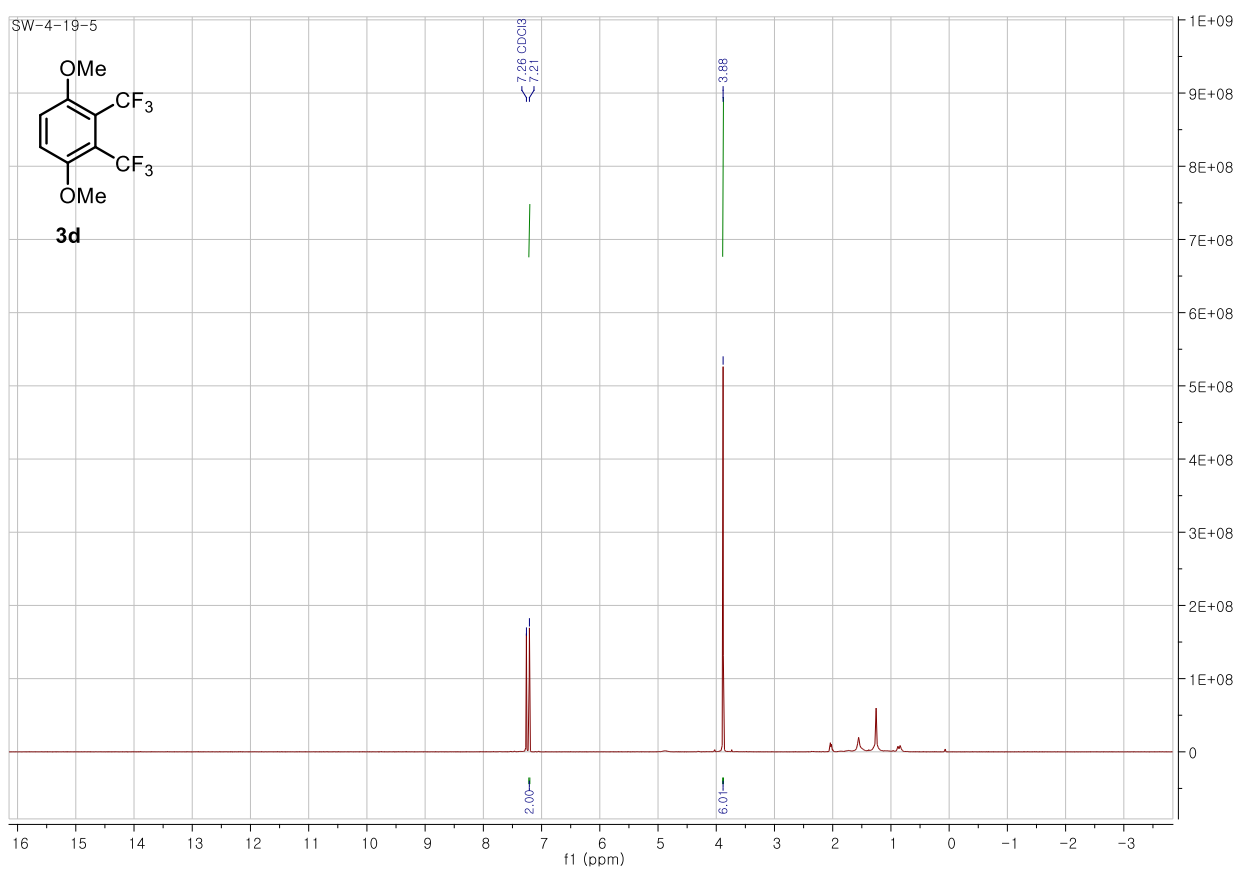
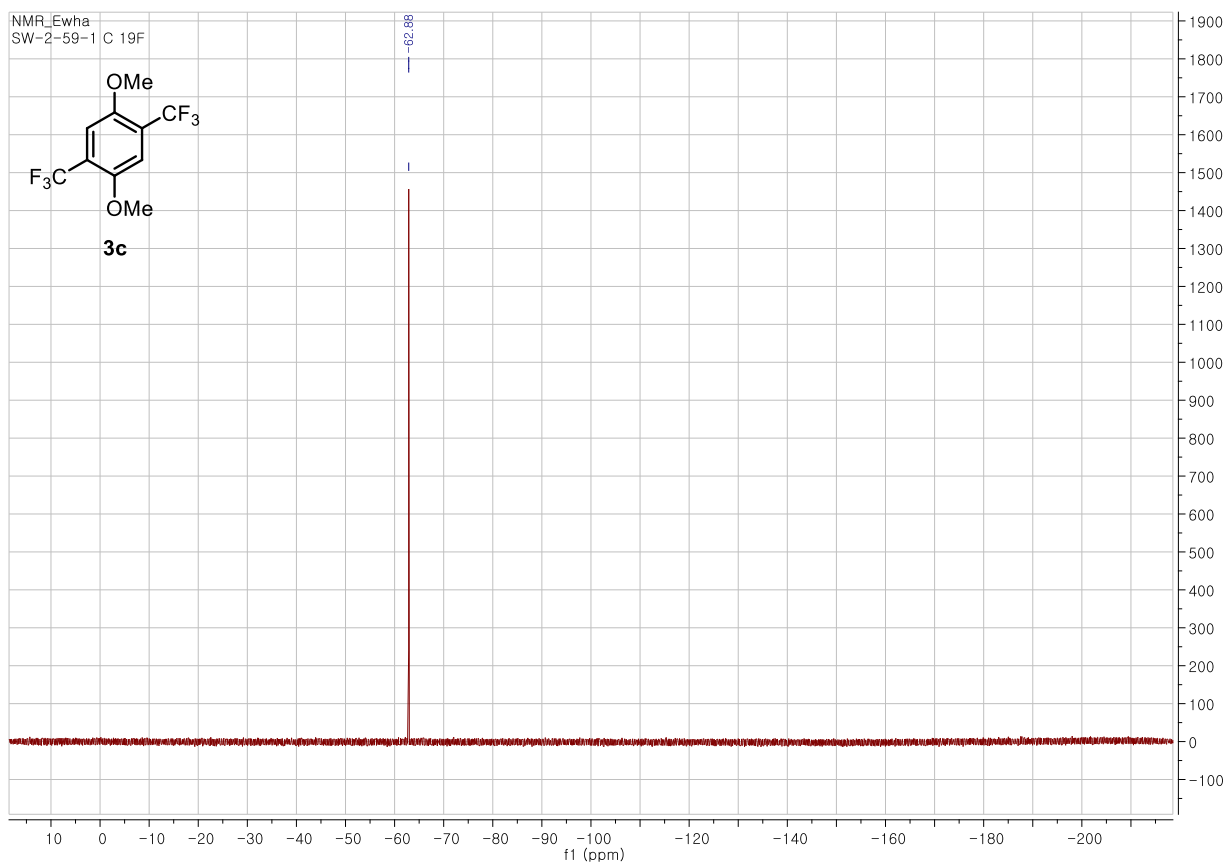


methyl 5-(2,5-dimethyl-4-(trifluoromethyl)phenoxy)-2,2-dimethylpentanoate (9). Identical to previously reported spectra.²³

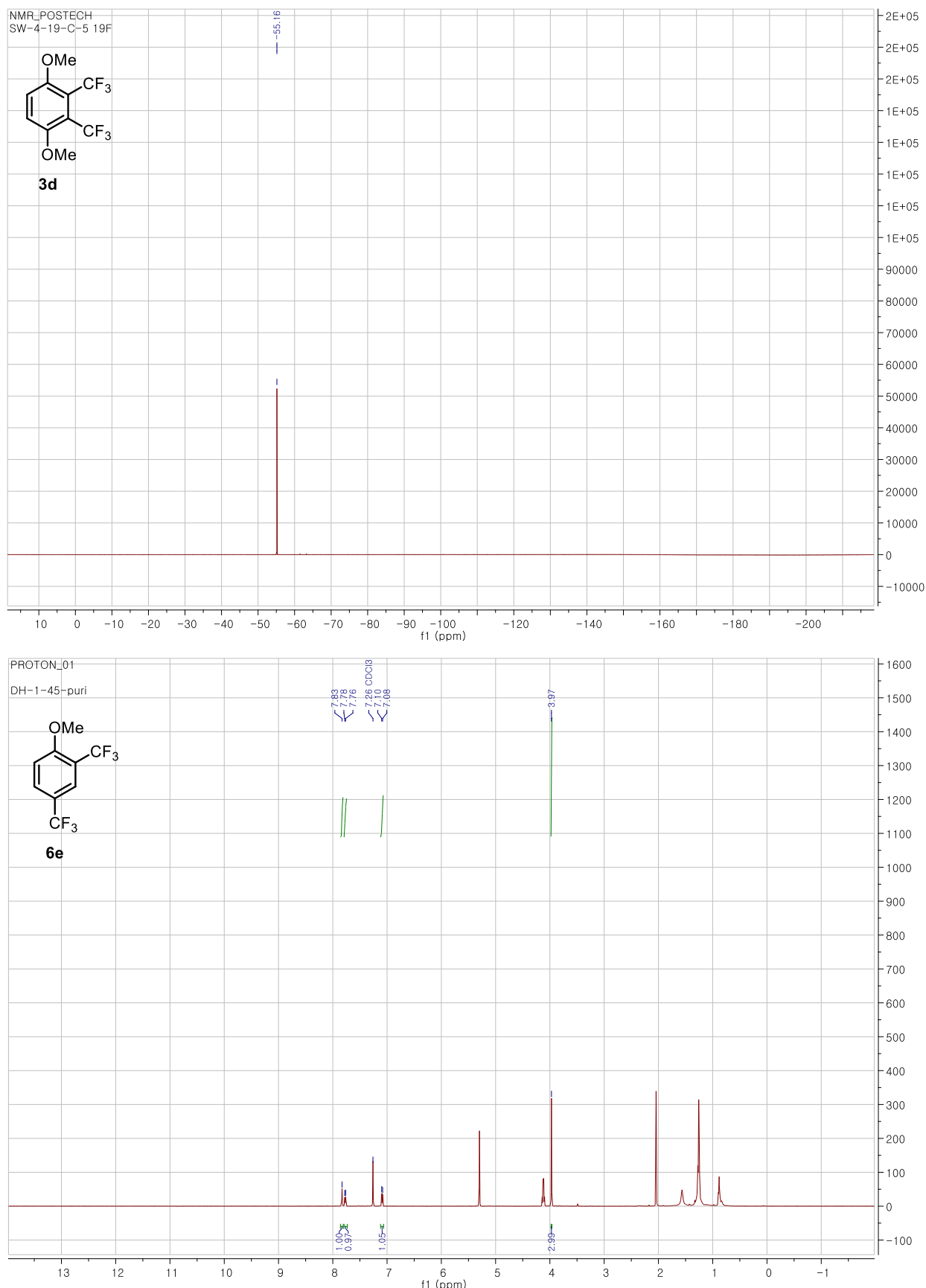
SUPPORTING INFORMATION



SUPPORTING INFORMATION

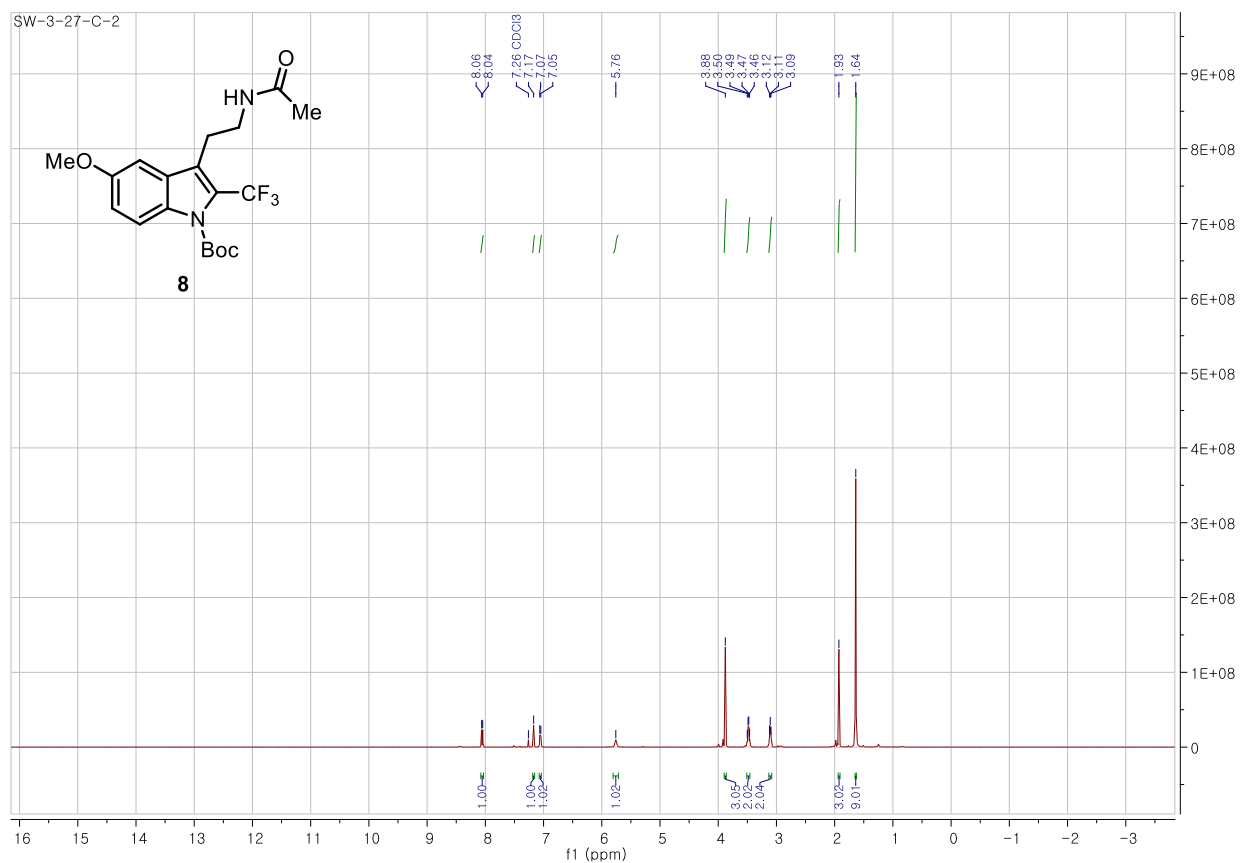
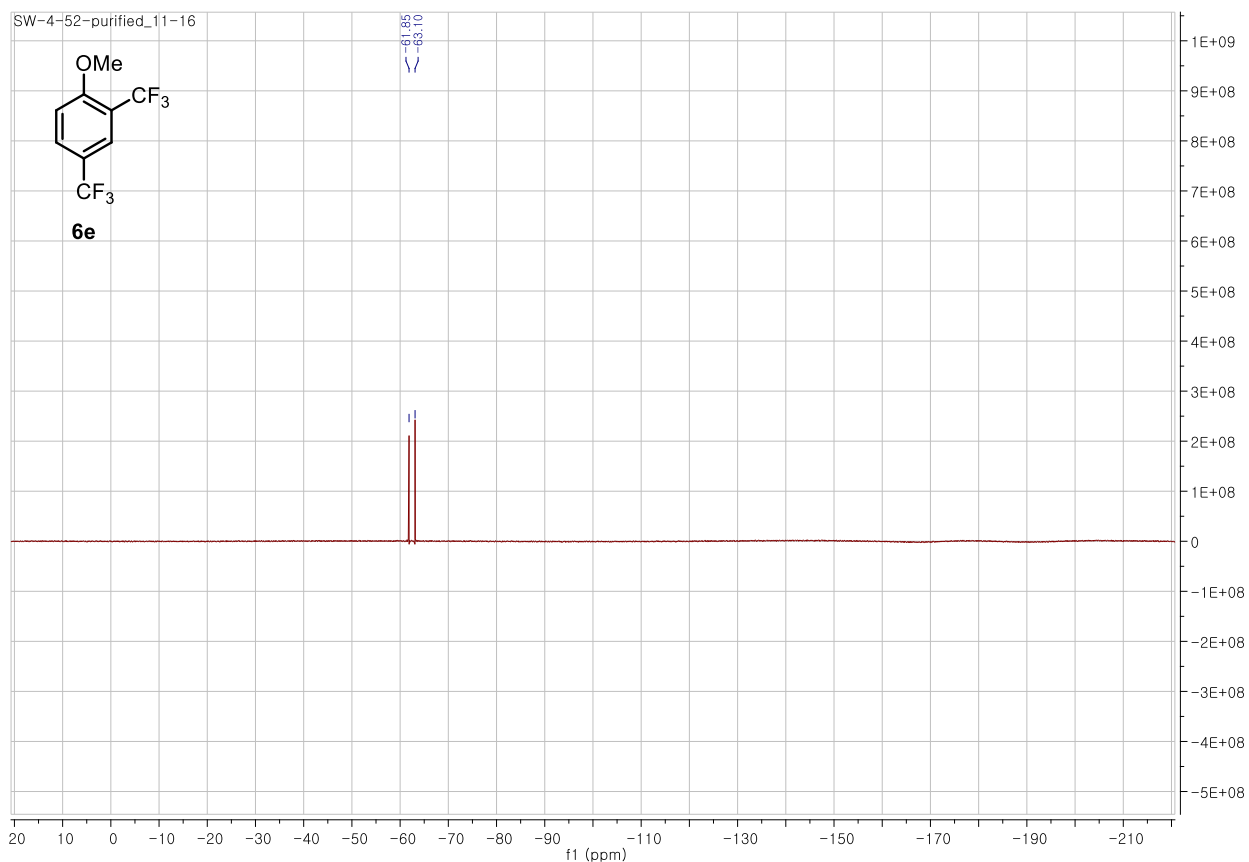


SUPPORTING INFORMATION

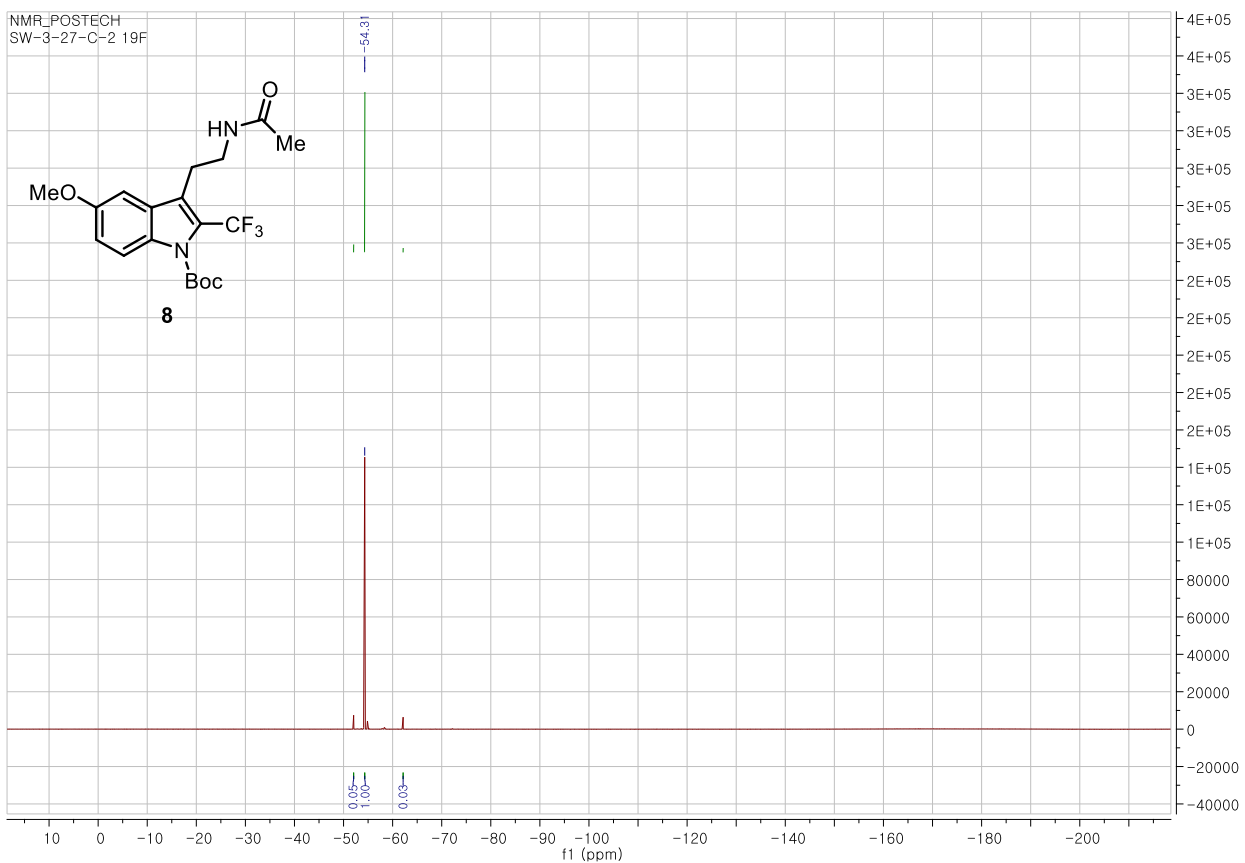
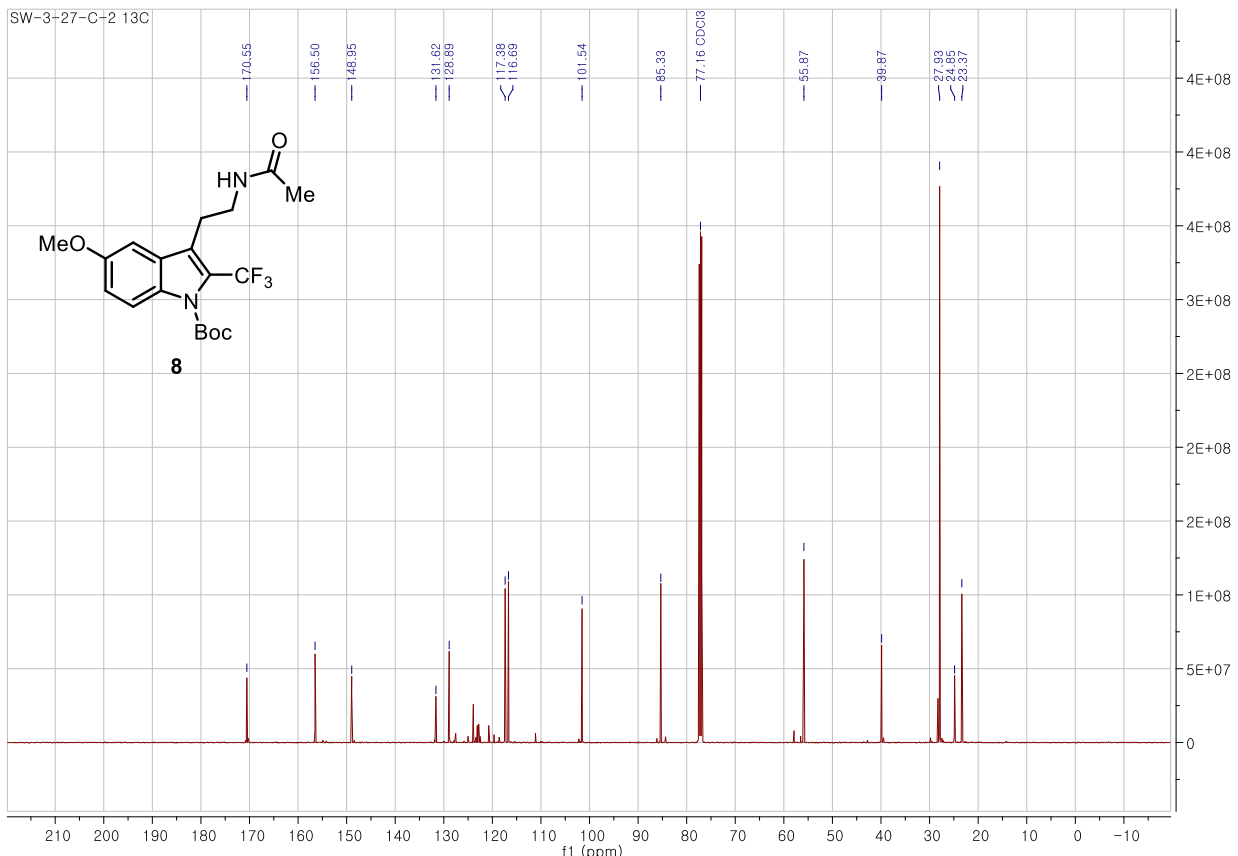


*Due to highly volatile nature of this compound, the solvent peaks (δ 5.30 (s) for dichloromethane, δ 4.12 (q) and δ 2.04 (s) for ethyl acetate) could not be fully removed. Yet, the compound peaks can be indubitably assigned.

SUPPORTING INFORMATION



SUPPORTING INFORMATION



SUPPORTING INFORMATION

References

- 1 Y. Ling, G. Wang, D. A. Wheeler, J. Z. Zhang and Y. Li, *Nano Lett.*, 2011, **11**, 2119–2125.
- 2 L. Vayssières, N. Beermann, S. E. Lindquist and A. Hagfeldt, *Chem. Mater.*, 2001, **13**, 233–235.
- 3 C. Lohaus, A. Klein and W. Jaegermann, *Nat. Commun.*, 2018, **9**, 4309.
- 4 M. Barroso, S. R. Pendlebury, A. J. Cowan and J. R. Durrant, *Chem. Sci.*, 2013, **4**, 2724–2734.
- 5 R. Van De Krol, Y. Liang and J. Schoonman, *J. Mater. Chem.*, 2008, **18**, 2311–2320.
- 6 A. G. Tamirat, J. Rick, A. A. Dubale, W. N. Su and B. J. Hwang, *Nanoscale Horizons*, 2016, **1**, 243–267.
- 7 Y. Shao, Z. Gan, E. Epifanovsky, A. T. B. Gilbert, M. Wormit, J. Kussmann, A. W. Lange, A. Behn, J. Deng, X. Feng, D. Ghosh, M. Goldey, P. R. Horn, L. D. Jacobson, I. Kaliman, R. Z. Khaliullin, T. Kuš, A. Landau, J. Liu, E. I. Proynov, Y. M. Rhee, R. M. Richard, M. A. Rohrdanz, R. P. Steele, E. J. Sundstrom, H. L. Woodcock, P. M. Zimmerman, D. Zuev, B. Albrecht, E. Alguire, B. Austin, G. J. O. Beran, Y. A. Bernard, E. Berquist, K. Brandhorst, K. B. Bravaya, S. T. Brown, D. Casanova, C. M. Chang, Y. Chen, S. H. Chien, K. D. Closser, D. L. Crittenden, M. Diedenhofen, R. A. Distasio, H. Do, A. D. Dutoi, R. G. Edgar, S. Fatehi, L. Fusti-Molnar, A. Ghysels, A. Golubeva-Zadorozhnaya, J. Gomes, M. W. D. Hanson-Heine, P. H. P. Harbach, A. W. Hauser, E. G. Hohenstein, Z. C. Holden, T. C. Jagau, H. Ji, B. Kaduk, K. Khistyaev, J. Kim, J. Kim, R. A. King, P. Klunzinger, D. Kosenkov, T. Kowalczyk, C. M. Krauter, K. U. Lao, A. D. Laurent, K. V. Lawler, S. V. Levchenko, C. Y. Lin, F. Liu, E. Livshits, R. C. Lochan, A. Luenser, P. Manohar, S. F. Manzer, S. P. Mao, N. Mardirossian, A. V. Marenich, S. A. Maurer, N. J. Mayhall, E. Neuscamman, C. M. Oana, R. Olivares-Amaya, D. P. O'Neill, J. A. Parkhill, T. M. Perrine, R. Peverati, A. Prociuk, D. R. Rehn, E. Rosta, N. J. Russ, S. M. Sharada, S. Sharma, D. W. Small, A. Sodt, T. Stein, D. Stück, Y. C. Su, A. J. W. Thom, T. Tsuchimochi, V. Vanovschi, L. Vogt, O. Vydrov, T. Wang, M. A. Watson, J. Wenzel, A. White, C. F. Williams, J. Yang, S. Yeganeh, S. R. Yost, Z. Q. You, I. Y. Zhang, X. Zhang, Y. Zhao, B. R. Brooks, G. K. L. Chan, D. M. Chipman, C. J. Cramer, W. A. Goddard, M. S. Gordon, W. J. Hehre, A. Klamt, H. F. Schaefer, M. W. Schmidt, C. D. Sherrill, D. G. Truhlar, A. Warshel, X. Xu, A. Aspuru-Guzik, R. Baer, A. T. Bell, N. A. Besley, J. Da Chai, A. Dreuw, B. D. Dunietz, T. R. Furlani, S. R. Gwaltney, C. P. Hsu, Y. Jung, J. Kong, D. S. Lambrecht, W. Liang, C. Ochsenfeld, V. A. Rassolov, L. V. Slipchenko, J. E. Subotnik, T. Van Voorhis, J. M. Herbert, A. I. Krylov, P. M. W. Gill and M. Head-Gordon, *Mol. Phys.*, 2015, **113**, 184–215.
- 8 Y. S. Lin, G. De Li, S. P. Mao and J. Da Chai, *J. Chem. Theory Comput.*, 2013, **9**, 263–272.
- 9 P. C. Hariharan and J. A. Pople, *Theor. Chim. Acta*, 1973, **28**, 213–222.
- 10 A. W. Lange and J. M. Herbert, *J. Phys. Chem. Lett.*, 2010, **1**, 556–561.
- 11 F. Weigend and R. Ahlrichs, *Phys. Chem. Chem. Phys.*, 2005, **7**, 3297–3305.
- 12 Y. Huang, R. J. Nielsen, W. A. Goddard and M. P. Soriaga, *J. Am. Chem. Soc.*, 2015, **137**, 6692–6698.
- 13 L. Li, X. Mu, W. Liu, Y. Wang, Z. Mi and C. J. Li, *J. Am. Chem. Soc.*, 2016, **138**, 5809–5812.
- 14 E. A. Meucci, S. N. Nguyen, N. M. Camasso, E. Chong, A. Arifafard, A. J. Carty and M. S. Sanford, *J. Am. Chem. Soc.*, 2019, **141**, 12872–12879.
- 15 Y. Deng, F. Lu, S. You, T. Xia, Y. Zheng, C. Lu, G. Yang, Z. Chen, M. Gao and A. Lei, *Chinese J. Chem.*, 2019, **37**, 817–820.
- 16 Y. Ye, S. H. Lee and M. S. Sanford, *Org. Lett.*, 2011, **13**, 5464–5467.
- 17 S. Hunig, R. Bau, M. Kemmer, H. Meixner, T. Metzenthin, K. Peters, K. Singzger and J. Gulbis, *European J. Org. Chem.*, 1998, **2**, 335–348.
- 18 S. Deolka, R. Govindarajan, E. Khaskin, R. R. Fayzullin, M. C. Roy and J. R. Khusnutdinova, *Angew. Chem. Int. Ed.*, 2021, **60**, 24620–24629.
- 19 F. Eisenreich and A. R. A. Palmans, *Chem. Eur. J.*, 2022, **28**, e202201322.
- 20 X. Yang and G. C. Tsui, *Chem. Sci.*, 2018, **9**, 8871–8875.
- 21 S. Mizuta, I. S. R. Stenhammar, M. O'Duill, J. Wolstenholme, A. K. Kirjavainen, S. J. Forsback, M. Tredwell, G. Sandford, P. R. Moore, M. Huiban, S. K. Luthra, J. Passchier, O. Solin and V. Gouverneur, *Org. Lett.*, 2013, **15**, 2648–2651.
- 22 G. Shi, C. Shao, S. Pan, J. Yu and Y. Zhang, *Org. Lett.*, 2015, **17**, 38–41.
- 23 F. Ye, F. Berger, H. Jia, J. Ford, A. Wortman, J. Borgel, C. Genicot and T. Ritter, *Angew. Chem. Int. Ed.*, 2019, **58**, 14615–14619.
- 24 T. Umemoto and A. Ando, *Bull. Chem. Soc. Jpn.* **1986**, **59**, 447–452.
- 25 Z. Zuchun, C. Xin, W. Jianchao, S. Hongbin, and L. J. Shih-Chieh, Alpha-(trifluoromethyl-substituted aryloxy, arylamino, arylthio or arylmethyl)-trifluoromethyl-substituted phenylacetic acid and derivatives as antidiabetic agents. WO2005080340A1, September 1, 2005.